Supplementary Materials

Enhanced corrosion resistance of eco-friendly MXene composite coating with self-healing performances

Xiaoqing Ma, Tiange Wang, Baolong Gong, Jiale Hou, Shuxian Ji, Huaijie Cao*

Shanghai Key Laboratory of Materials Protection and Advanced Materials in Electric Power, Shanghai Engineering Research Center of Energy-Saving in Heat Exchange Systems, College of Environmental and Chemical Engineering, Shanghai University of Electric Power, Shanghai, 200090, China.

Dr. Huaijie Cao

Shanghai Key Laboratory of Materials Protection and Advanced Materials in Electric Power, Shanghai Engineering Research Center of Energy-Saving in Heat Exchange Systems, College of Environmental and Chemical Engineering, Shanghai University of Electric Power, Shanghai, 200090, China.

Email: **hjcao0510@shiep.edu.cn**

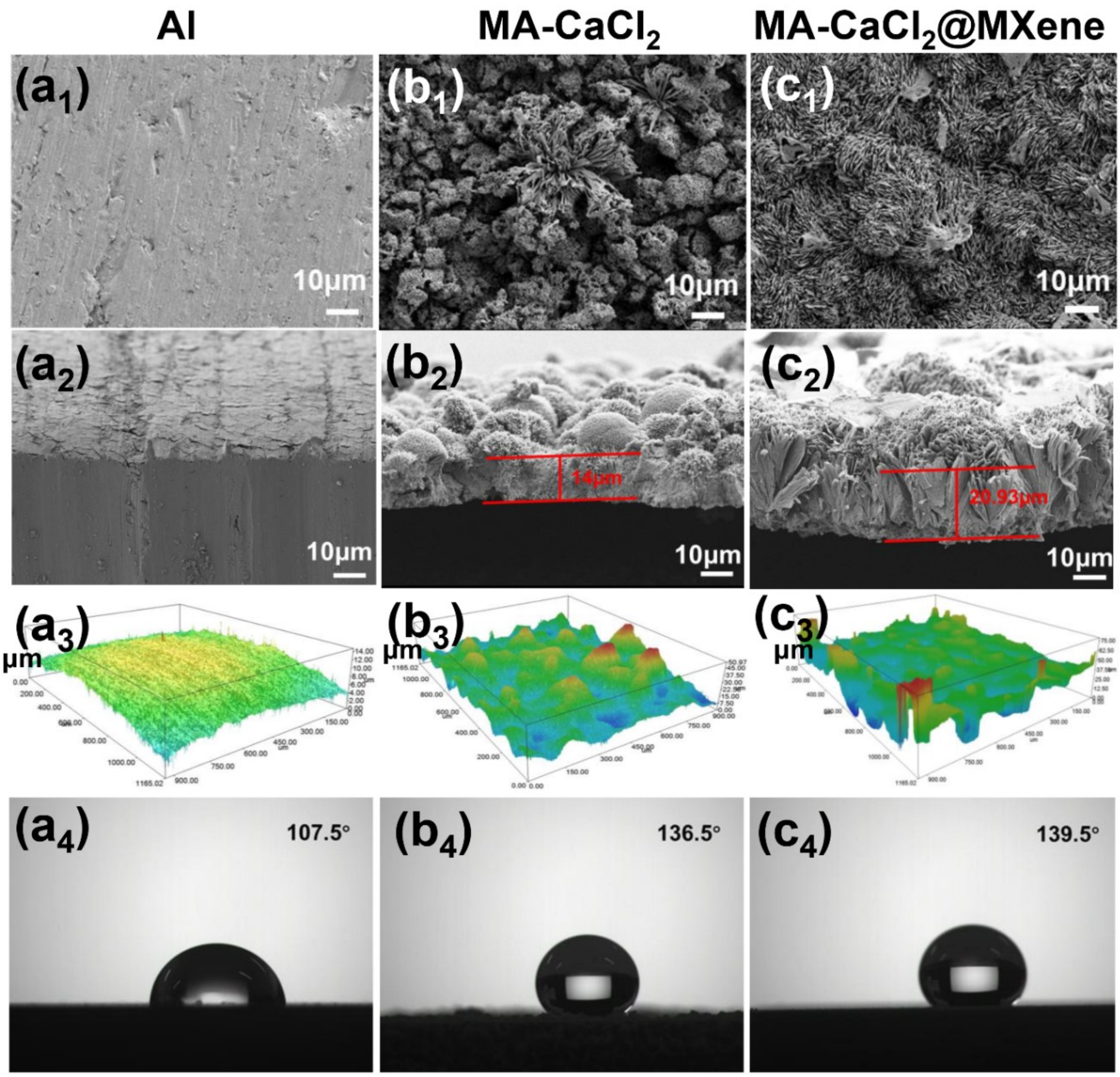

Fig. S1. SEM images, Cross-sectional SEM images, 3D morphologies, and water contact angle of the samples: (a_1-a_4) Al, (b_1-b_4) $(C_{13}H_{27}COO)_2Ca$, and (c_1-c_4) $(C_{13}H_{27}COO)_2Ca$@MXene coating.

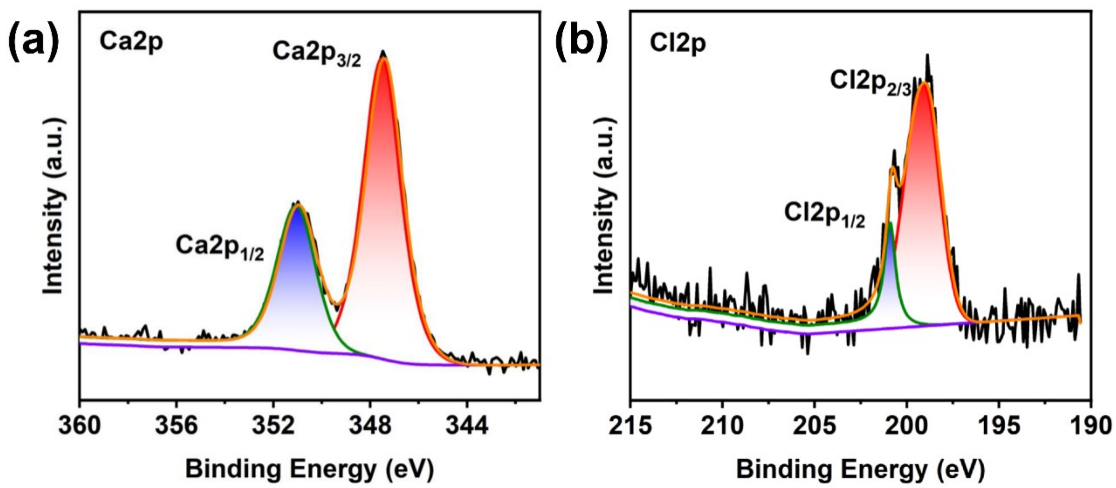

Fig. S2. XPS spectra of $(C_{13}H_{27}COO)_2Ca$-TA@MXene coating: (a) Ca2p, (b) Cl2p.

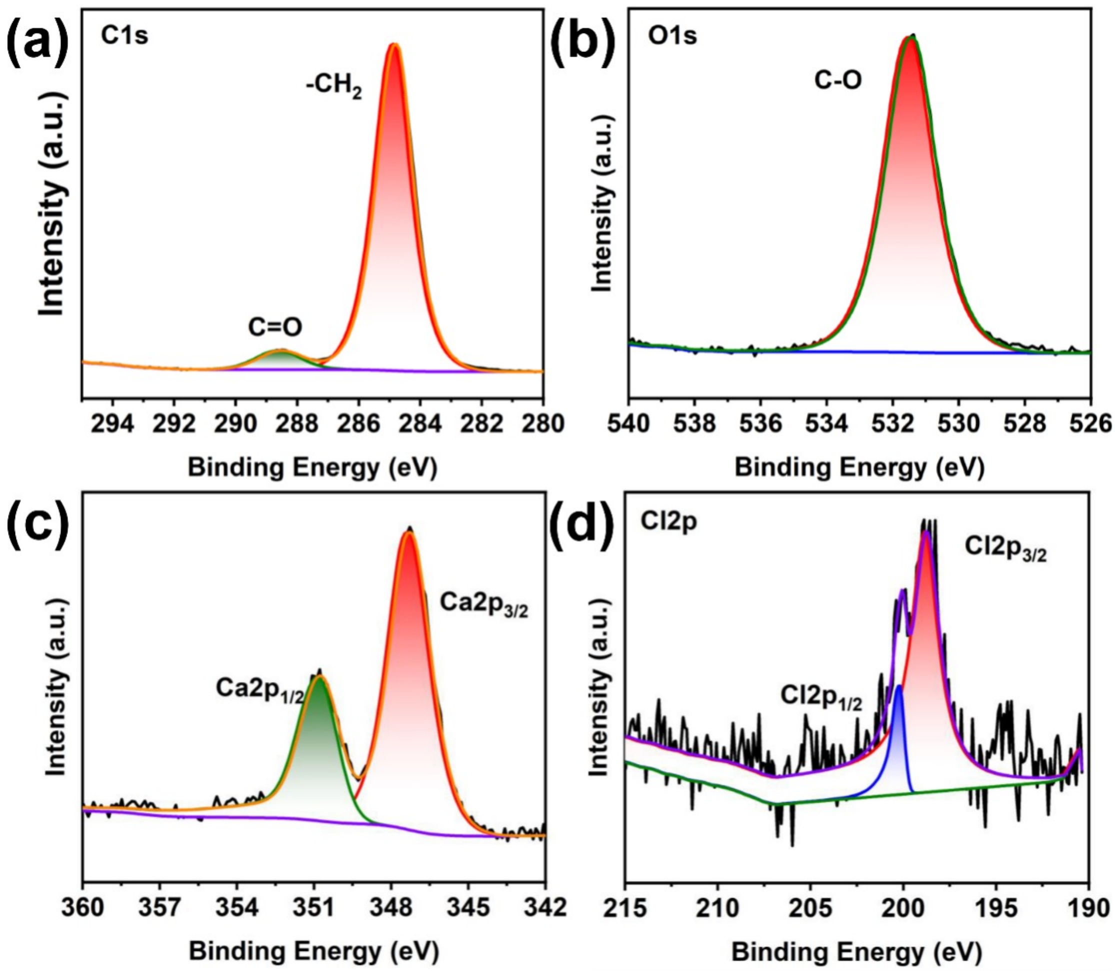

Fig. S3. XPS spectra of $(C_{13}H_{27}COO)_2Ca$ coating: (a) C1s, (b) O1s, (c) Ca2p, (d) Cl2p.

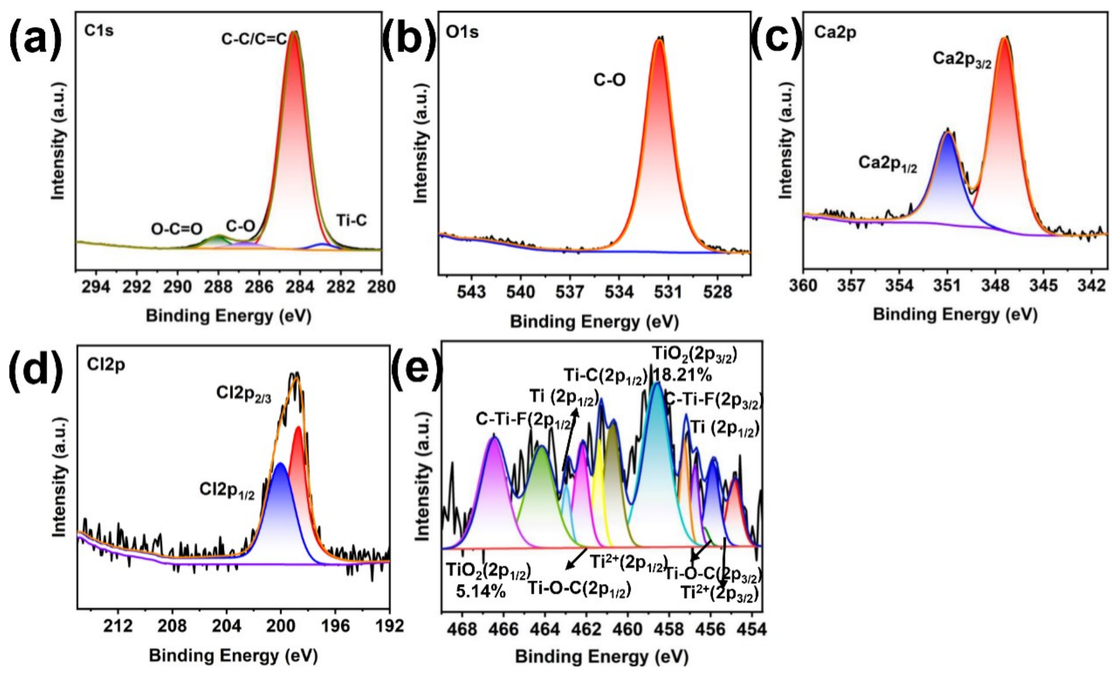

Fig. S4. XPS spectra of $(C_{13}H_{27}COO)_2Ca$@MXene coating: (a) C1s, (b) O1s, (c) Ca2p, (d) Cl2p, (e) Ti2p.

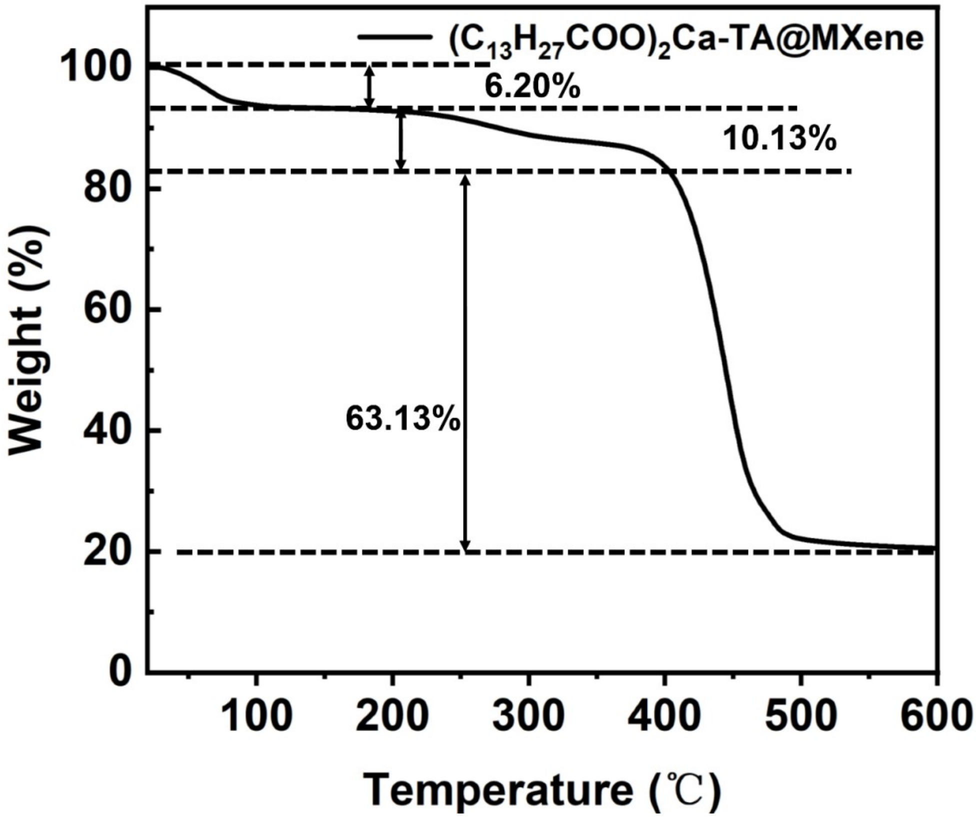

Fig. S5. TGA curve of $(C_{13}H_{27}COO)_2Ca$-TA@MXene composite coating under nitrogen atmosphere.

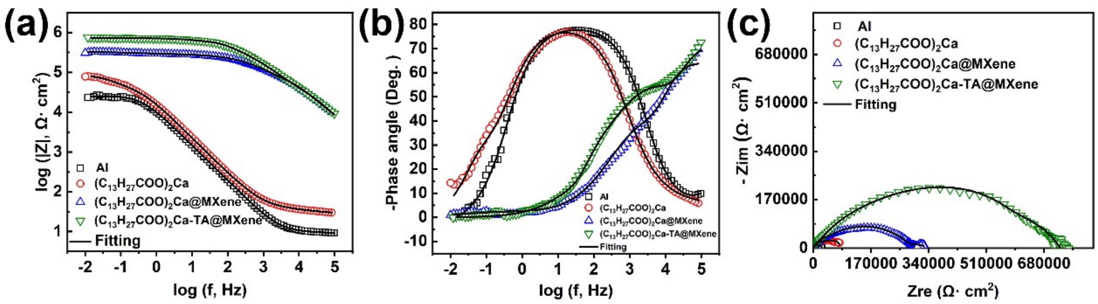

Fig. S6. (a) Bode plots, (b) phase angle plots, and (c) Nyquist plots of the various coatings in 3.5 wt.% NaCl solution.

Table S1. Electrochemical parameters obtained from the EIS plots of the different samples.

Sample	R_s(Ω)	R_c (Ω)	CPE_1		L(H)	CPE_{dl}		L(H)	R_1(Ω)	C(F)	R_{ct} (Ω)
			Y_0 (S.cm^{-2}.s^n)	n		Y_0 (S.cm^{-2}.s^n)	n				
Al alloy	0.01	9.689	1.545 ×10^{-6}	0.6944	/	1.83× 10^{-5}	0.883	2.639 ×10^4	3.381× 10^4	0.0002071	2268

$(C_{13}H_{27}COO)_2Ca$ sample	29.95	2.166×10^{4}	1.708×10^{-5}	0.922	/	3.412×10^{-5}	0.8179	0.01175	6.415×10^{4}	1.822×10^{-6}	7.808
$(C_{13}H_{27}COO)_2Ca$@MXene sample	1000	5.401×10^{4}	1.587×10^{-5}	0.4718	/	2.319×10^{-8}	0.6586	/	2.608×10^{5}	8.06×10^{-10}	2.038×10^{4}
$(C_{13}H_{27}COO)_2Ca$-TA@MXene sample	0.01958	6.887×10^{5}	1.334×10^{-8}	0.7107	/	6.611×10^{-10}	1	/	1×10^{4}	3.191×10^{-9}	2.105×10^{4}

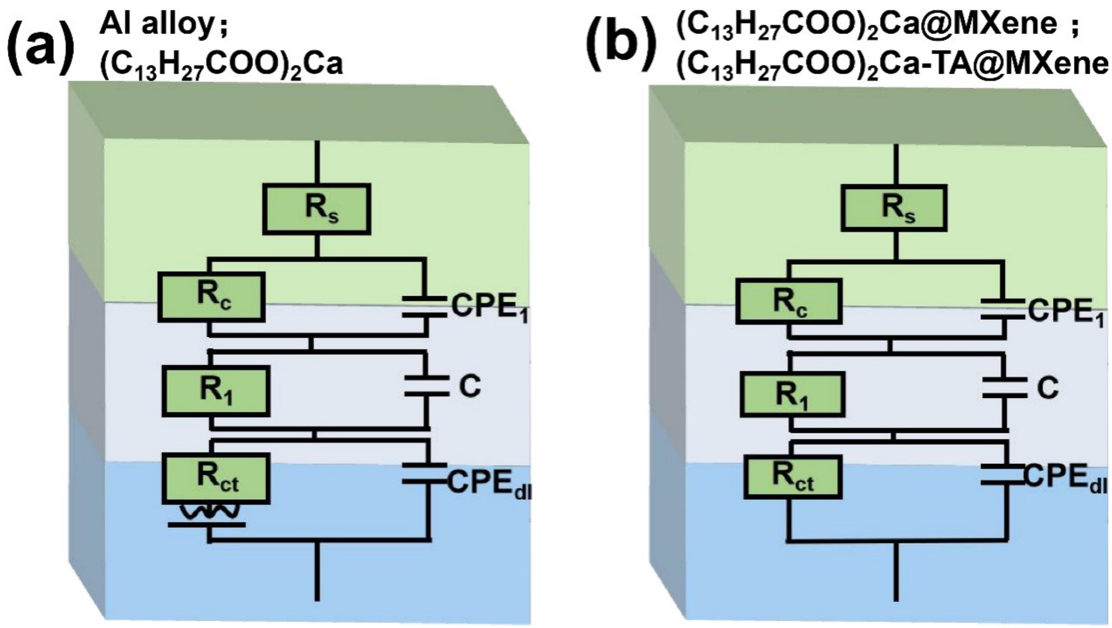

Fig. S7. Equivalent circuit models of different samples.

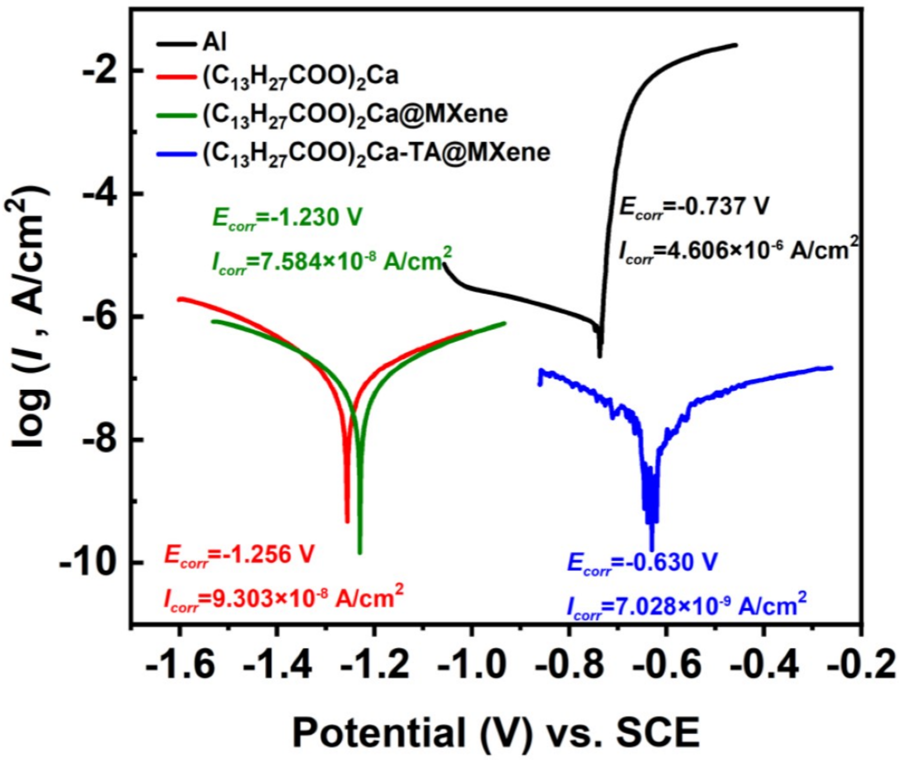

Fig. S8. Potentiodynamic polarization curves of the various coatings in 3.5 wt.% NaCl solution.

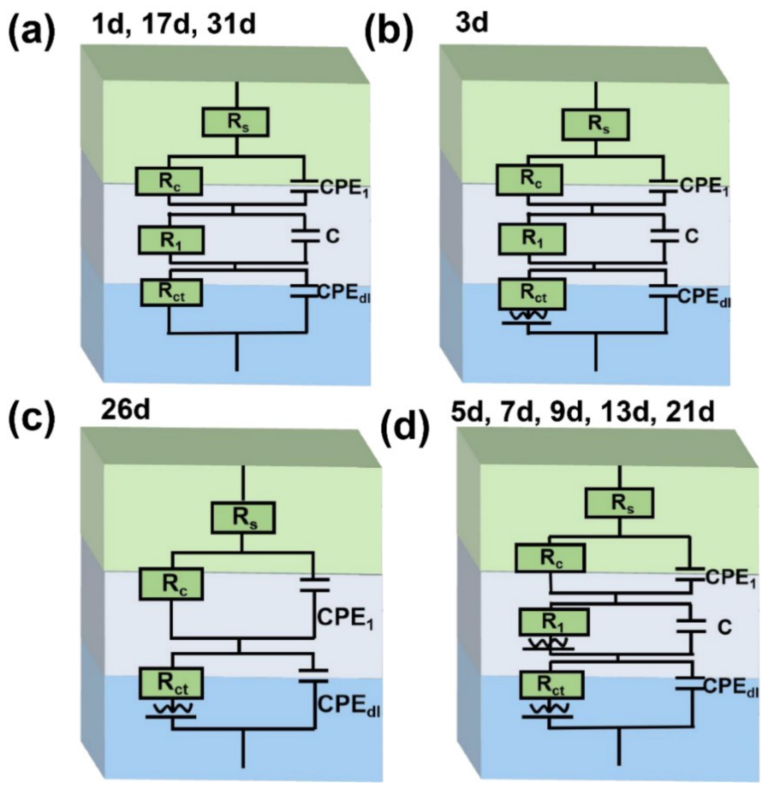

Fig. S9. Equivalent circuit model of bare Al.

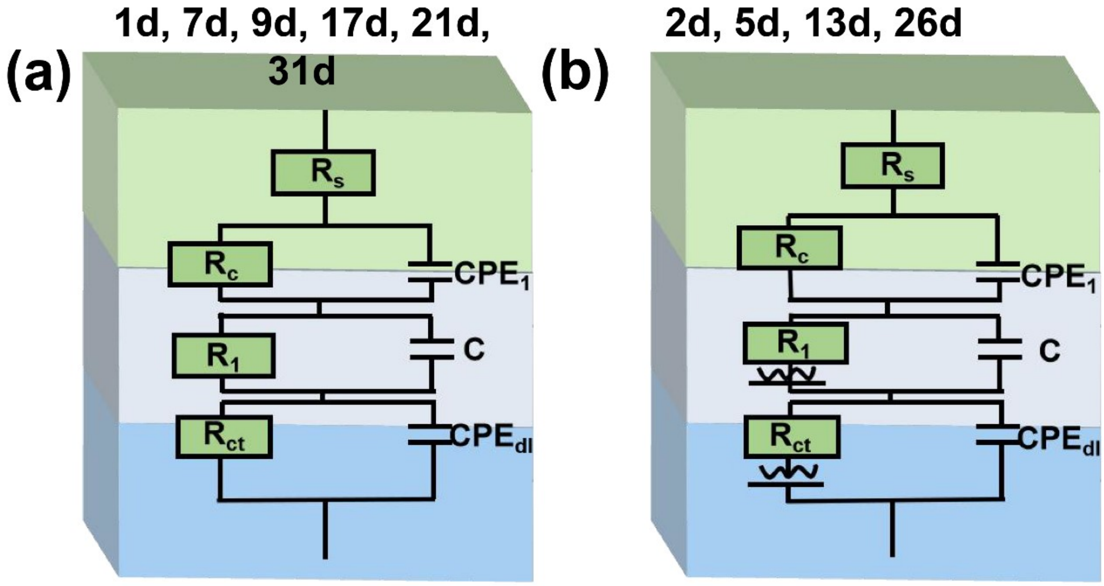

Fig. S10. Equivalent circuit model of $(C_{13}H_{27}COO)_2Ca$.

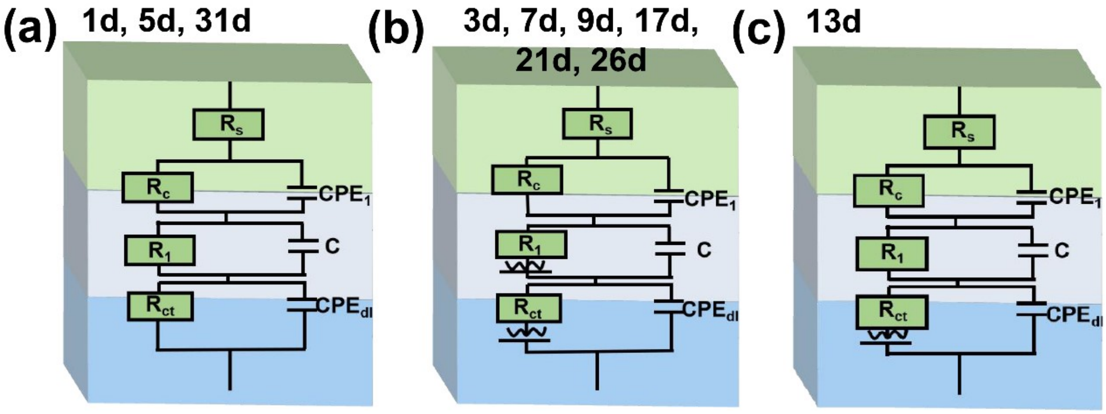

Fig. S11. Equivalent circuit model of $(C_{13}H_{27}COO)_2Ca$@MXene.

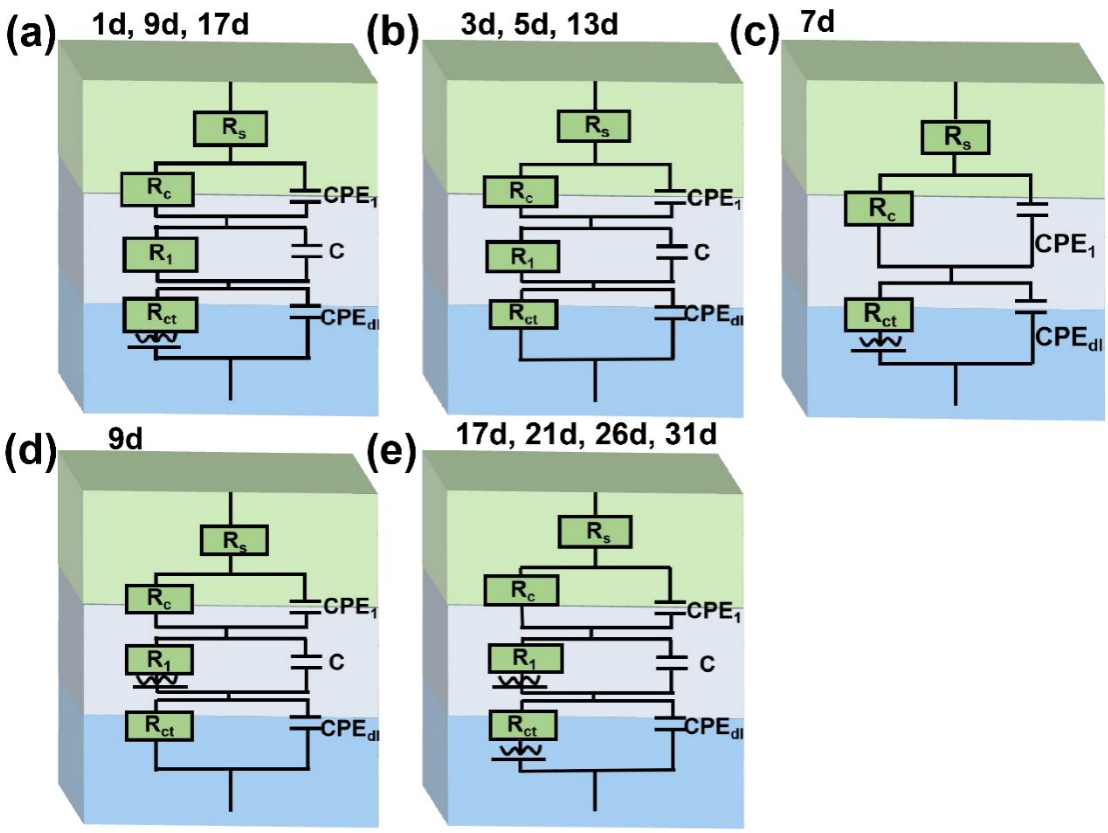

Fig. S12. Equivalent circuit model of $(C_{13}H_{27}COO)_2Ca$-TA@MXene.

Table S2. Electrochemical parameters obtained from the EIS plots of Al alloy during the immersion tests.

Sample	R_s (Ω)	R_c (Ω)	CPE$_1$ Y_0 ($S.cm^{-2}.s^n$)	CPE$_1$ n	L(H)	CPE$_{dl}$ Y_0 ($S.cm^{-2}.s^n$)	CPE$_{dl}$ n	L(H)	R_1(Ω)	C (F)	R_{ct} (Ω)
1d	3.021×10^4	471.7	1.092×10^{-5}	0.8996	/	7.284×10^{-6}	0.6388	/	5.446×10^4	1.932×10^6	847.6
3d	1.792	1.707×10^4	2.357×10^{-5}	0.8584	/	1.833×10^{-6}	0.7332	6122	7.651	3.16×10^{-5}	3.611×10^4
5d	2.76	4.85×10^4	1.471×10^{-5}	0.8874	153.2	5.639×10^{-6}	0.6763	12.07	7.075	14.97	1.06×10^4
7d	7.435	1.092×10^4	1.06×10^{-5}	0.8994	2.893×10^9	1.224×10^{-5}	0.8736	3.449×10^4	2.753	4.207×10^{-5}	3.076×10^4
9d	0.02	2.0	1.681×	0.8	1.59×1	1.129	0.5	7.22×	10.51	0.000363	2.726

	038	79×10^{4}	10^{-5}	954	0^{5}	$\times10^{-5}$	638	10^{12}		4	$\times10^{4}$
13d	0.2124	6907	6.599×10^{-5}	1	5.35	0.0007899	0.5717	1.803	3.909×10^{16}	1.301×10^{-5}	8068
17d	5.443	2.754×10^{4}	0.007199	0.8	/	1.566×10^{-5}	0.9039	/	2.304×10^{11}	0.001183	1.805×10^{4}
21d	14.6	2.595×10^{4}	0.0001297	0.6815	0.001593	2.501×10^{-6}	0.8375	3.23×10^{4}	7.946	1.606×10^{-5}	1.027×10^{4}
26d	2.258	1.271×10^{4}	1.793×10^{-5}	0.8856	/	5.827×10^{-6}	0.6524	0.01418	/	/	7.04
31d	11.24	1.708×10^{4}	1.767×10^{-5}	0.9135	/	0.0007973	0.6479	7.497×10^{14}	1.799×10^{9}	0.02869	383.7

Table S3. Electrochemical parameters obtained from the EIS plots of the $(C_{13}H_{27}COO)_2Ca$ coating during the immersion tests.

Sample	**R_s(Ω)**	**R_c(Ω)**	**CPE_1**		**L(H)**	**CPE_{dl}**		**L(H)**	**R_1(Ω)**	**C(F)**	**R_{ct}(Ω)**
			Y_0 ($S.cm^{-2}.s^n$)	**n**		**Y_0 ($S.cm^{-2}.s^n$)**	**n**				
1d	1	7675	8.083×10^{-5}	0.3852	/	3.373×10^{-9}	0.8972	/	0.06699	0.001646	5801
3d	10	9479	3.731×10^{-7}	0.598	6.492×10^{17}	7.963×10^{-6}	0.7392	2.936	660.6	0.002835	6663
5d	0.05316	1.428×10^{4}	2.092×10^{-6}	0.513	2.902×10^{5}	1.651×10^{-5}	0.7732	3.283	347.7	0.0008582	2.385×10^{4}
7d	1000	1.434×10^{4}	2.071×10^{-5}	0.8183	/	5.831×10^{-6}	0.631	/	145.5	0.00131	1.026×10^{4}
9d	0.01	2.405×10^{4}	1.777×10^{-5}	0.8844	/	0.0002016	0.2473	/	91.96	0.1079	1.04×10^{4}
13d	34.48	4.215×10^{4}	2.959×10^{-5}	0.6834	5.35	1.33×10^{-6}	0.5911	0.2652	425.5	2.819×10^{-6}	66.2
17d	10	9.9	4.611×	0.7	/	2.874	0.3	/	385	3.457×10	1.087

		82×10^{4}	10^{-5}	174		$\times10^{-5}$	794			$^{-5}$	$\times10^{4}$
21d	0.01	2.757×10^{4}	6.495×10^{-5}	0.668	/	0.0003904	0.3663	/	329.2	2.963×10^{-5}	7308
26d	0.01	2.824×10^{4}	3.185×10^{-5}	0.7075	0.856	3.668×10^{-5}	0.3808	0.01342	207.4	4.878×10^{-6}	15.56
31d	14.02	3.778×10^{4}	2.268×10^{-5}	0.8238	/	7.23×10^{-5}	0.3467	/	206.8	9.177×10^{-5}	3.128×10^{4}

Table S4. Electrochemical parameters obtained from the EIS plots of the $(C_{13}H_{27}COO)_2Ca$@MXene coating during the immersion tests.

Sample	R_s (Ω)	R_c (Ω)	CPE_1		L(H)	CPE_{dl}		L(H)	R_1(Ω)	C(F)	R_{ct}(Ω)
			Y_0 ($S.cm^{-2}.s^n$)	n		Y_0 ($S.cm^{-2}.s^n$)	n				
1d	1259	2.442×10^{4}	4.326×10^{-8}	0.709	/	9.379×10^{-7}	0.6182	/	8.924×10^{4}	0.0001026	1.057×10^{4}
3d	61.56	1.775×10^{5}	1.872×10^{-9}	0.9548	1.178	4.14×10^{-6}	0.4584	4.602×10^{16}	2680	1.082×10^{-6}	1.555×10^{4}
5d	0.02299	1.521×10^{4}	3.156×10^{-9}	0.8	/	2.11×10^{-5}	0.8	/	1.226×10^{5}	1.377×10^{-5}	1560
7d	122.3	7.898×10^{4}	2.091×10^{-5}	0.4036	0.09502	9.621×10^{-8}	0.9132	1.092	285.3	1.693×10^{-9}	687.2
9d	198.2	3.586×10^{4}	2.955×10^{-5}	0.4321	1.313×10^{5}	1.652×10^{-8}	0.843	2.97	822.3	0.000156	4.714×10^{4}
13d	0.01	7.438×10^{4}	6.093×10^{-8}	0.7402	/	4.789×10^{-5}	0.3936	3.147×10^{7}	897.9	0.0004447	8307
17d	0.07636	7.108×10^{4}	3.72×10^{-5}	0.6272	17.64	3.189×10^{-5}	0.3501	0.866	0.866	6.499×10^{-9}	164.3
21d	0.02543	1.968×10^{4}	3.224×10^{-5}	0.7003	7.776×10^{4}	4.612×10^{-6}	0.461	123	368.2	0.0001216	3.605×10^{4}
26d	35.4	1.7	2.867×	0.6	4.438×	3.121	0.7	0.350	189.6	0.000114	2.891

	6	04×10^{4}	10^{-5}	668	10^{4}	$\times10^{-7}$	074	8		6	$\times10^{4}$
31d	0.01	3.823×10^{4}	2.064×10^{-5}	0.7483	/	0.0002209	0.552	/	202.7	0.0002761	2.983×10^{4}

Table S5. Electrochemical parameters obtained from the EIS plots of the $(C_{13}H_{27}COO)_2Ca$-TA@MXene coating during the immersion tests.

Sample	**R_s(Ω)**	**R_c(Ω)**	**CPE_1**		**L(H)**	**CPE_{dl}**		**L(H)**	**R_1(Ω)**	**C(F)**	**R_{ct}(Ω)**
			Y_0 ($S.cm^{-2}.s^n$)	**n**		**Y_0 ($S.cm^{-2}.s^n$)**	**n**				
1d	0.01	7.476×10^{4}	2.043×10^{-6}	0.6208	/	5.083×10^{-8}	0.6824	3.905×10^{4}	2.283×10^{4}	0.0006438	7.09×10^{4}
3d	100	1.402×10^{5}	3.497×10^{-5}	0.7184	/	1.801×10^{-6}	0.5335	/	370.7	2.963×10^{-5}	2.6×10^{5}
5d	0.01	4.187×10^{5}	2.114×10^{-5}	0.6475	/	1.67×10^{-7}	0.7659	/	1961	8.475×10^{-5}	1.209×10^{5}
7d	10	2.093×10^{5}	2.94×10^{-5}	0.7652	/	4.335×10^{-6}	0.4822	254.9	/	4.523×10^{-5}	2.035×10^{4}
9d	0.01	9.199×10^{4}	9.98×10^{-9}	0.883	1.76×10^{15}	4.151×10^{-5}	0.5686	/	497.3	1.967×10^{8}	8.02×10^{5}
13d	100	6.605×10^{4}	4.333×10^{-5}	0.4849	/	7.7732×10^{-8}	0.7574	/	380.1	3.322×10^{-5}	7.256×10^{4}
17d	0.0136	5.193×10^{4}	1.492×10^{-5}	0.4258	163.8	3.278×10^{-5}	0.636	3.13×10^{5}	252.2	0.00602	2.03×10^{4}
21d	0.01	5.973×10^{4}	0.000118	0.3285	3.318	2.403×10^{-5}	0.6746	7.818×10^{5}	33.1	0.0001116	1.992×10^{5}
26d	0.01	2.698×10^{5}	3.454×10^{-5}	0.5948	1.314	0.00149	0.3446	117.4	218	4.423×10^{-5}	1.2×10^{5}
31d	0.01	1.194×10^{5}	0.002494	0.8	1.235	2.201×10^{-5}	0.7139	1.205×10^{6}	5.81×10^{4}	0.0001394	1.231×10^{5}

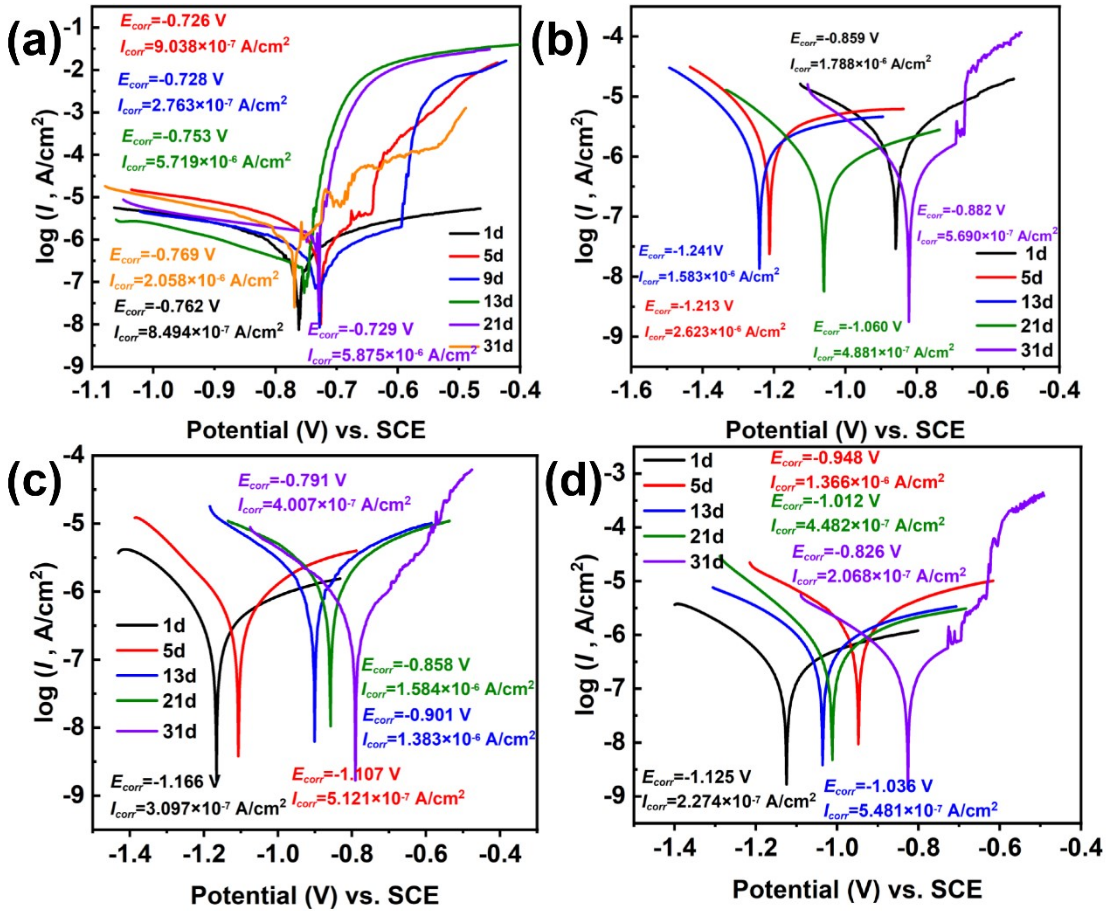

Fig. S13. Potentiodynamic polarization curves of (a) Al, (b) $(C_{13}H_{27}COO)_2Ca$, (c) $(C_{13}H_{27}COO)_2Ca$@MXene, and (d) $(C_{13}H_{27}COO)_2Ca$-TA@MXene coating versus immersion time.

Table S6. Comparison of various coatings in a simulated marine environment.

Sample	Corrosion solution	Self-healing efficiency (%)	Preparation time (h)	Thickness (μm)	Reference
Polyvinyl alcohol (PVA)/MXene@Fe_3O_4	3.5wt% NaCl	90.2	247	110±8	**[Ref. S1]**
Polyurethane- 1-(3-((N-n-butyl)aminecarboxamido)propyl)-3-hexadecyl imidazolidin bromide (PU-M16)	3.5wt% NaCl	97.17	60	55	**[Ref. S2]**
Polyaniline-benzotriazole (BTA)	3.5wt% NaCl	96	51	50±5	**[Ref. S3]**
Polyvinyl butyral @ gallic acid /epoxy (PVB@GA/EP)	3.5wt% NaCl	88.63	31	120±5	**[Ref. S4]**
Polyvinyl alcohol/ chitosan@ linseed oil/8-hydroxyquinone	3.5wt% NaCl	90.31	28	120±5	**[Ref. S5]**

(PVA/CS@LO/8-HQ)					
2-mecapobenzothiazole-loaded halloysite nanotube@ Polycaprolactone/epoxy (HNTs-MBT@PCL/EP)	3.5wt% NaCl	92	36	52	**[Ref. S6]**
Polydopamine@ benzotriazole/epoxy (PDA@BTA/EP)	3.5wt% NaCl	80.05	105	50±5	**[Ref. S7]**
Benzotriazole @ linseed oil /epoxy (BTA@LO/EP)	3.5wt% NaCl	98	172	400	**[Ref. S8]**
8-hydroxyquinone@ polyaniline (8-HQ@PANI)	3.5wt% NaCl	83.56	25	75±5	**[Ref. S9]**
Epoxy/2- benzotriazole / halloysite clay nanotubes (EP/2-BTA/HNTs)	3.5wt% NaCl	90	168	80±10	**[Ref. S10]**
This work	3.5wt% NaCl	99.53	1.77	21.59	**This work**

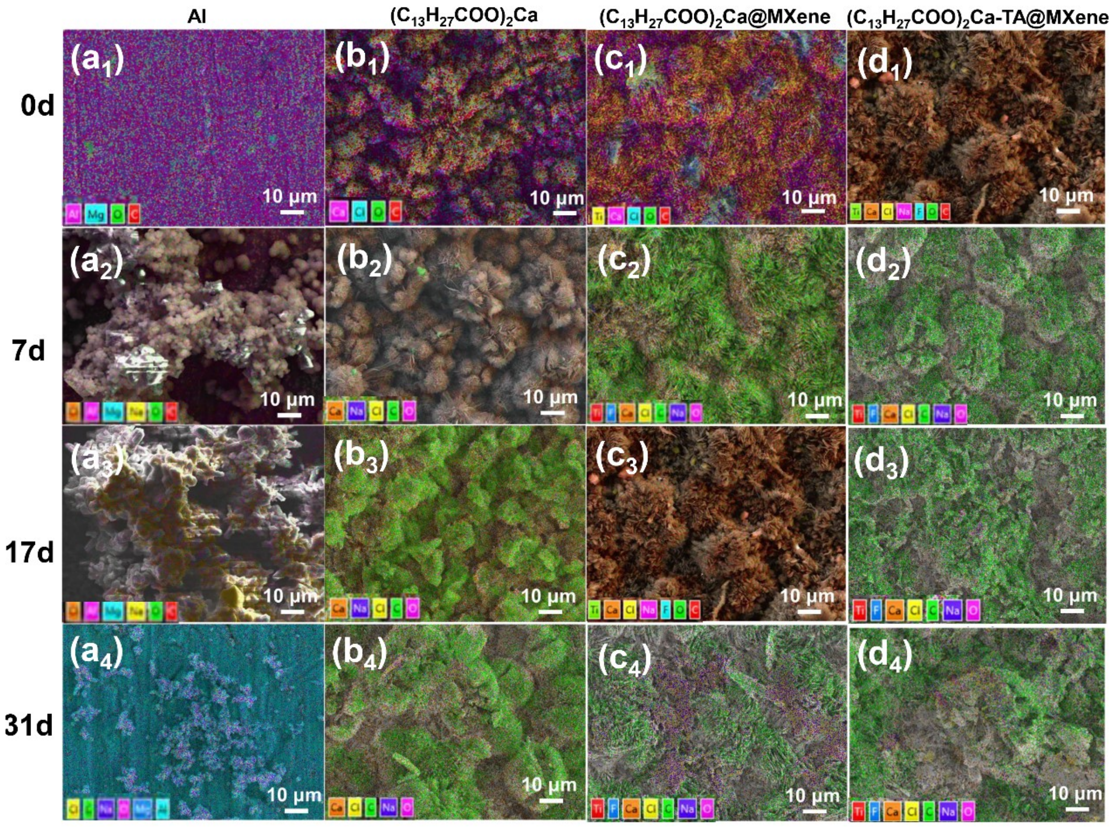

Fig. S14. EDS mappings of various samples versus different immersion time (0d, 7d, 17 d, and 31 d): (a_1-a_4) Al, (b_1-b_4) $(C_{13}H_{27}COO)_2Ca$, (c_1-c_4) $(C_{13}H_{27}COO)_2Ca$@MXene, and (d_1-d_4) $(C_{13}H_{27}COO)_2Ca$-TA@MXene coating.

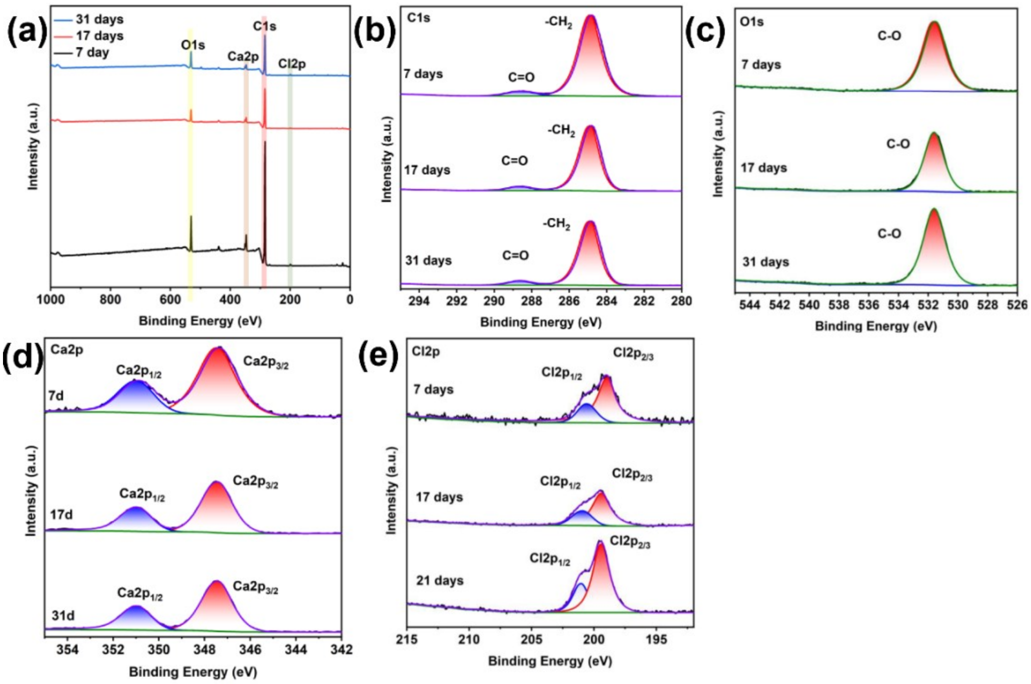

Fig. S15. XPS spectra of $(C_{13}H_{27}COO)_2Ca$ coating after immersion in 3.5wt% NaCl solution: (a) Survey spectrum, (b) C1s, (c) O1s, (d) Ca2p, (e) Cl2p.

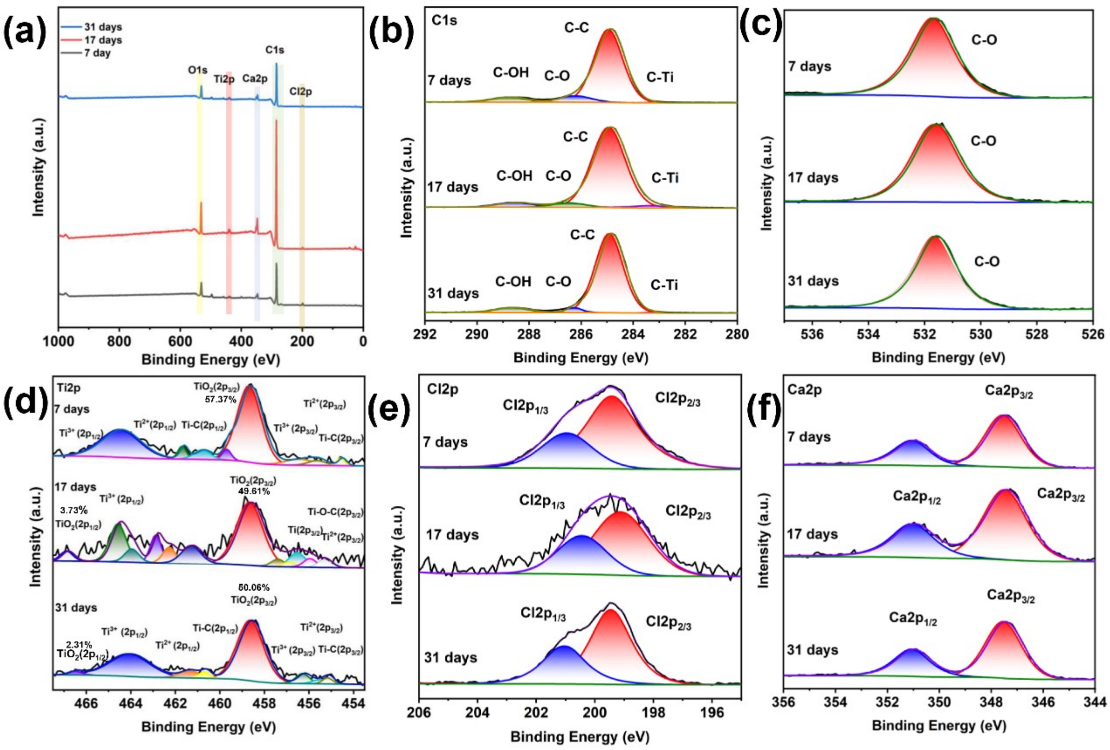

Fig. S16. XPS spectra of $(C_{13}H_{27}COO)_2Ca$@MXene coating after immersion in 3.5wt% NaCl solution: (a) Survey spectrum, (b) C1s, (c) O1s, (d) Ca2p, (e) Cl2p, (f) Ca2p.

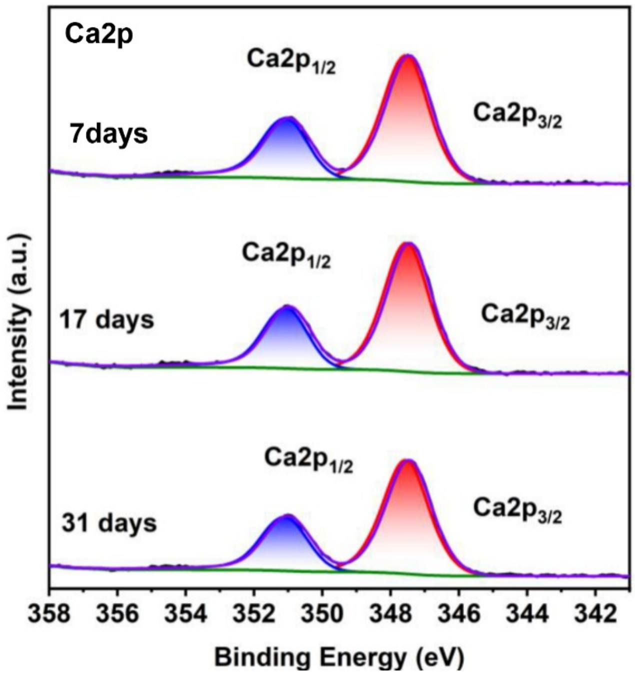

Fig. S17. XPS spectra of $(C_{13}H_{27}COO)_2Ca$-TA@MXene Ca2p after immersion in 3.5wt.% NaCl solution.

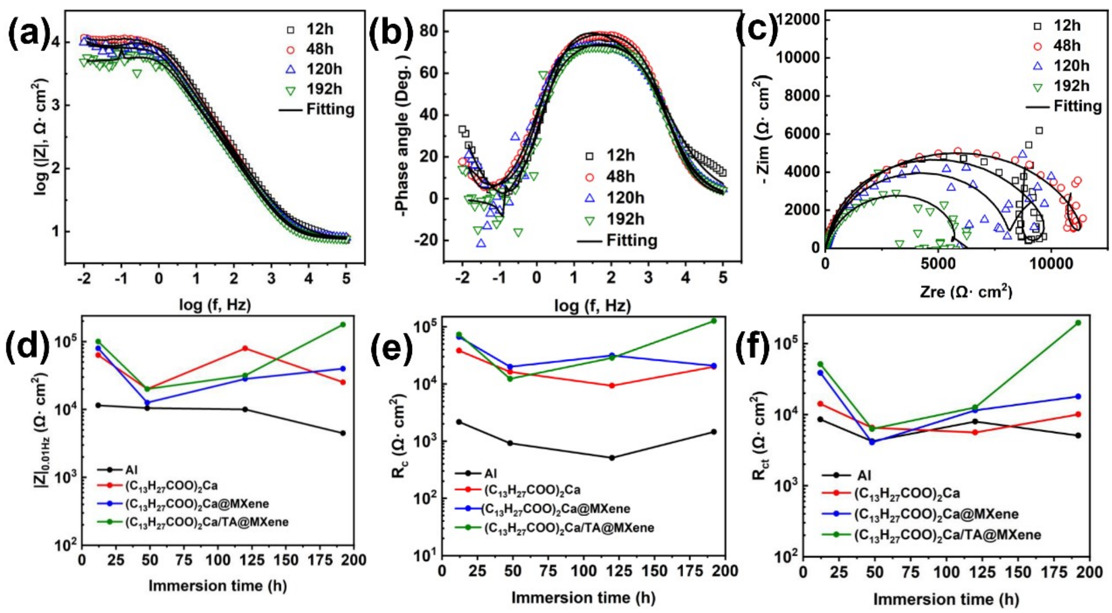

Fig. S18. (a) Nyquist plots, (b) Bode impedance plots, (c) Bode phase plots of the artificially scratched Al after immersion in 3.5wt% NaCl solution, the (d) $|Z|_{0.01Hz}$, (e) R_c, and (f) R_{ct} of artificially scratched Al, $(C_{13}H_{27}COO)_2Ca$, $(C_{13}H_{27}COO)_2Ca$@MXene, and $(C_{13}H_{27}COO)_2Ca$-TA@MXene samples versus different immersion time.

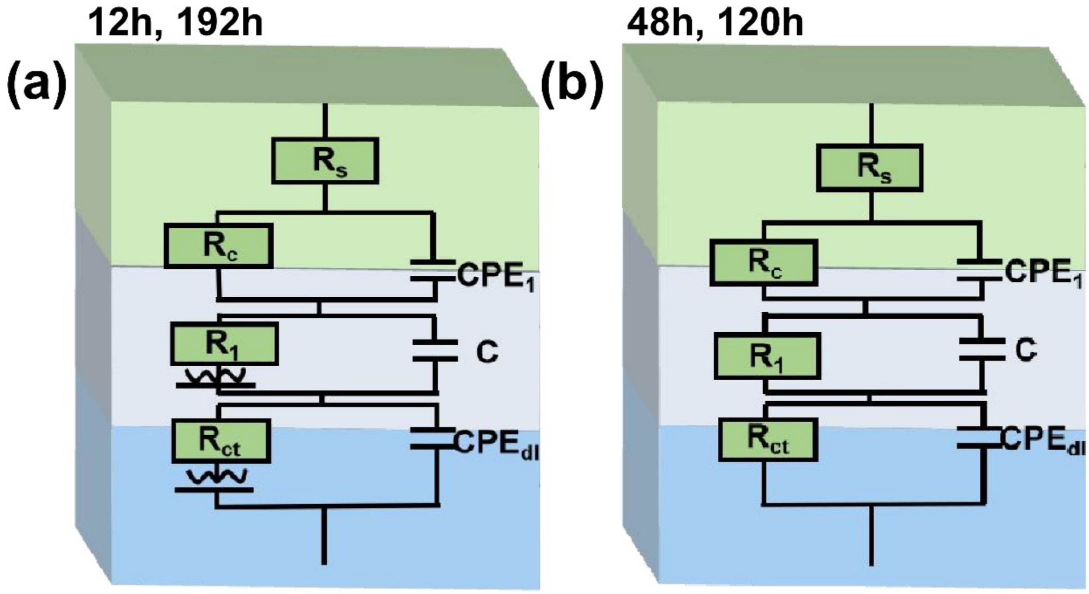

Fig. S19. Equivalent circuit model of the scratched Al alloy versus the immersion time..

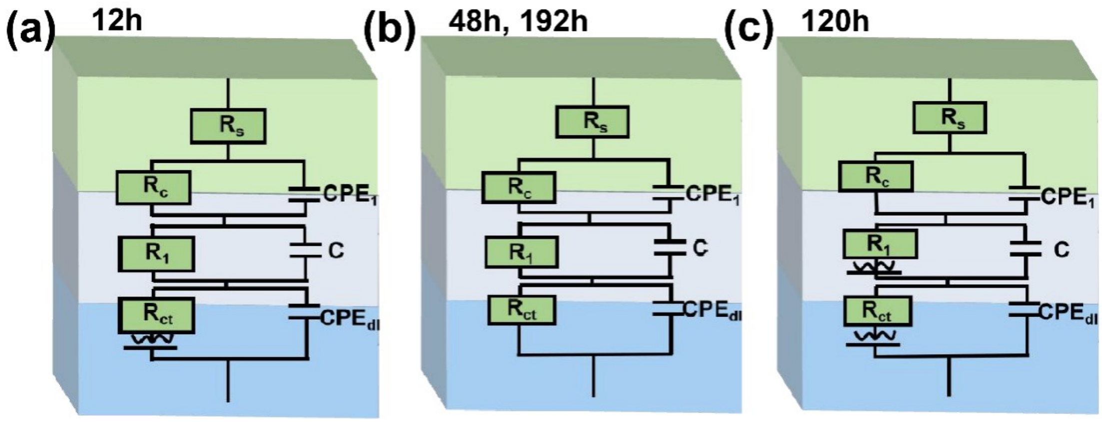

Fig. S20. Equivalent circuit model of the scratched $(C_{13}H_{27}COO)_2Ca$ coating versus the immersion time.

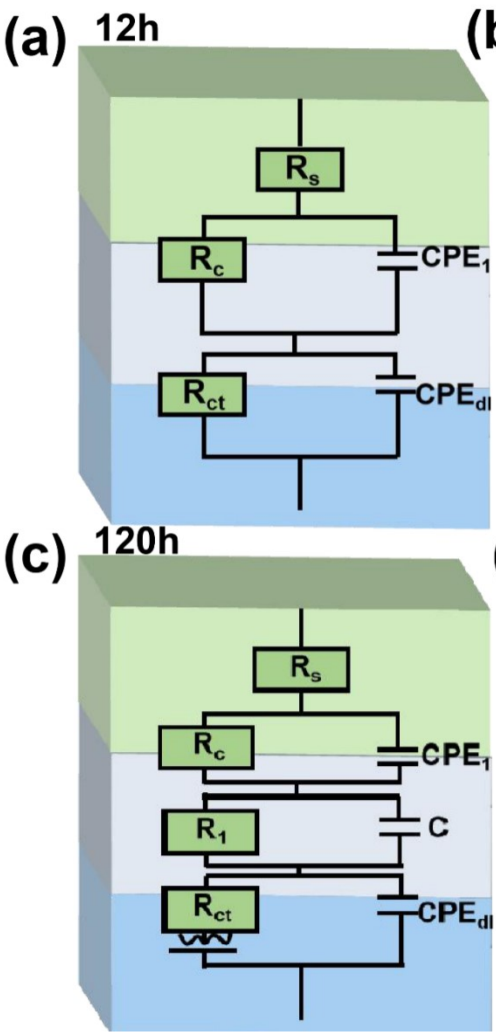

Fig. S21. Equivalent circuit model of the scratched $(C_{13}H_{27}COO)_2Ca$@MXene coating versus the immersion time.

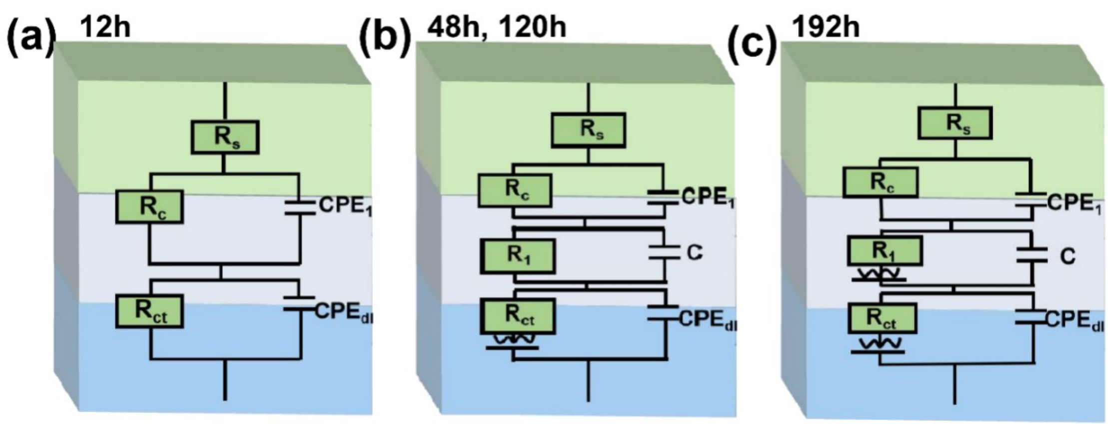

Fig. S22. Equivalent circuit model of the scratched $(C_{13}H_{27}COO)_2Ca$-TA@MXene coating versus the immersion time.

Table S7. Electrochemical parameters obtained from the EIS plots of the scratched Al alloy versus the immersion time.

Sample	R_s(Ω)	R_c(Ω)	CPE_1/CPE_P		L(H)	CPE_{dl}		L(H)	R_1(Ω)	C_1(F)	R_{ct}(Ω)
			Y_0 ($S.cm^{-2}.s^n$)	n		Y_0 ($S.cm^{-2}.s^n$)	n				
12h	3.441	2165	0.0003869	0.5826	1286	0.002271	0.9576	2.466×10^{14}	6.419×10^{18}	1.072×10^{-5}	8527
48h	8.285	918.6	5.182×10^{-5}	0.8005	/	1.071×10^{-5}	1	/	1.935×10^{4}	1.684×10^{10}	4204
120h	0.1619	509.4	5.972×10^{-9}	0.9353	/	9.404×10^{-5}	0.7536	/	7.872	1.79×10^{-5}	7964
192h	7.526	1452	0.0001956	0.7298	2325	2.658×10^{-5}	0.9222	30.04	5.663×10^{4}	0.008431	5052

Table S8. Electrochemical parameters obtained from the EIS plots of the scratched $(C_{13}H_{27}COO)_2Ca$ coating versus the immersion time.

Sample	R_s(Ω)	R_c(Ω)	CPE_1		L(H)	CPE_{dl}		L(H)	R_1(Ω)	C_1(F)	R_{ct}(Ω)
			Y_0 ($S.cm^{-2}.s^n$)	n		Y_0 ($S.cm^{-2}.s^n$)	n				
12h	141.8	3.822×10^{4}	3.978×10^{-5}	0.3232	/	1.425×10^{-6}	0.8386	1.066×10^{4}	8100	2.496×10^{6}	1.412×10^{4}
48h	0.01	1.629×10^{4}	1.078×10^{-5}	0.5265	/	1.108×10^{-6}	0.7044	/	501.6	0.003098	6516
120h	0.01	9318	1.01×10^{-5}	0.4998	226	5.985×10^{-9}	0.8331	1377	9.401×10^{4}	2.957×10^{-9}	5589
192h	74.29	2.001×10^{4}	2.226×10^{-5}	0.8	/	1.23×10^{-7}	0.8	/	640.2	0.00143	1.004×10^{4}

Table S9. Electrochemical parameters obtained from the EIS plots of the scratched $(C_{13}H_{27}COO)_2Ca$@MXene coating versus the immersion time.

Sampl	R	R_c(	CPE_1	L(H)	CPE_{dl}	L(H)	R_1(Ω)	C(F)	R_{ct}(Ω

e	s(Ω)	Ω)	Y_0 ($S.cm^{-2}.s^n$)	n		Y_0 ($S.cm^{-2}.s^n$)	n				)
12h	10	6.643×10^4	1.261×10^{-5}	0.4204	/	8.309×10^{-7}	0.4679	/	/	/	3.855×10^4
48h	0.6935	1.997×10^4	0.0001161	0.482	/	2.041×10^{-6}	0.6132	2.054×10^4	/	/	4050
120h	46.28	3.142×10^4	5.532×10^{-5}	0.8	/	9.759×10^{-7}	0.8	/	137.9	4.845×10^{-5}	1.145×10^4
192h	51.09	2.077×10^4	2.814×10^{-5}	0.7157	7.159×10^{19}	4.791×10^{-7}	0.867	0.2952	147.9	0.0002204	1.793×10^4

Table S10. Electrochemical parameters obtained from the EIS plots of the scratched $(C_{13}H_{27}COO)_2Ca$-TA@MXene coating versus the immersion time.

Sample	R_s(Ω)	R_c(Ω)	CPE_1		L(H)	CPE_{dl}		L(H)	R_1(Ω)	C(F)	R_{ct}(Ω)
			Y_0 ($S.cm^{-2}.s^n$)	n		Y_0 ($S.cm^{-2}.s^n$)	n				
12h	100	7.304×10^4	9.196×10^{-7}	0.5024	/	3.663×10^{-5}	0.4575	/	/	/	5.112×10^4
48h	3.935×10^4	1.226×10^4	9.576×10^{-7}	0.6361	/	6.034×10^{-5}	0.5118	2.054×10^4	1090	0.004631	6248
120h	8.164	2.858×10^4	2.671×10^{-6}	0.5903	/	4.109×10^{-5}	0.6981	3.825×10^{13}	297.5	0.002202	1.259×10^4
192h	10	1.262×10^5	1.223×10^{-6}	0.4966	4.982×10^5	2.224×10^{-9}	0.8655	274.6	2.53×10^4	2.258×10^{-5}	1.953×10^5

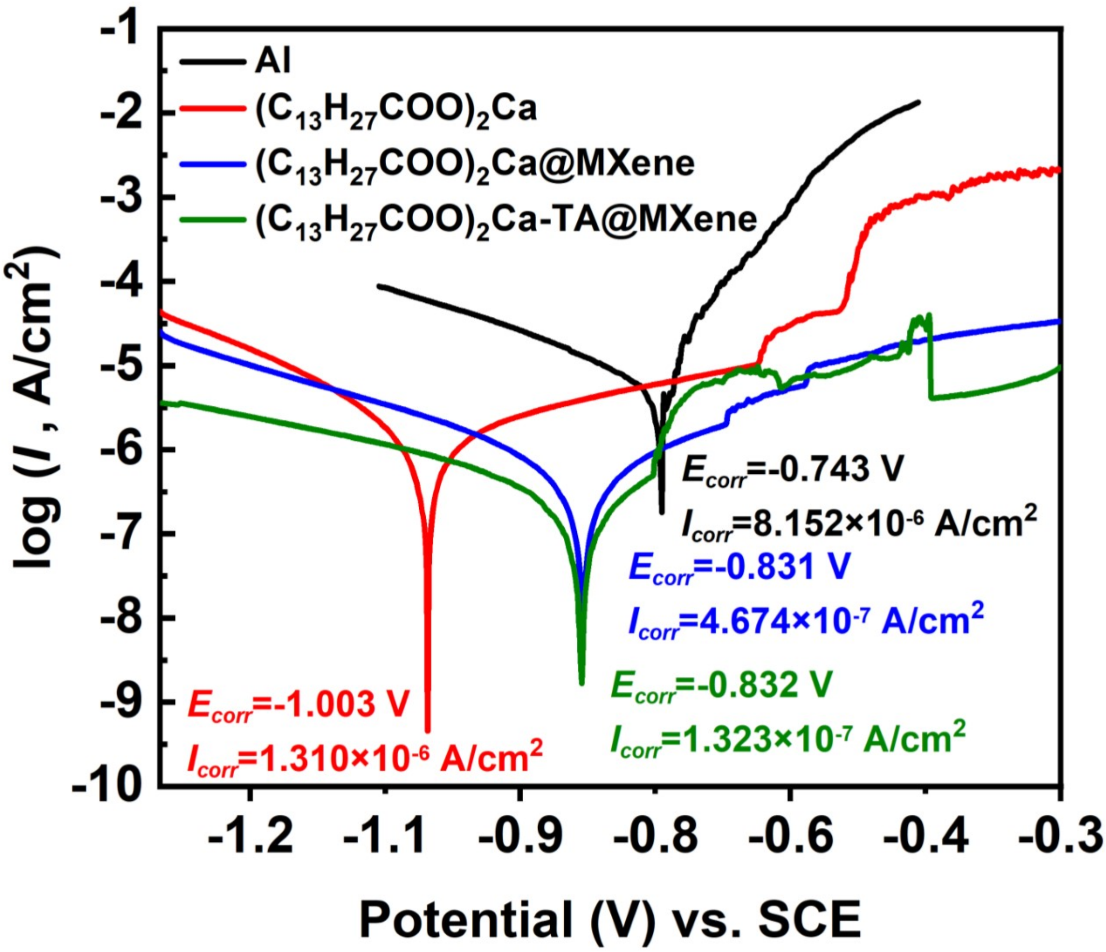

Fig. S23. Polarization curves of the scratched Al, $(C_{13}H_{27}COO)_2Ca$, $(C_{13}H_{27}COO)_2Ca$ @MXene, $(C_{13}H_{27}COO)_2Ca$-TA@MXene samples after immersion tests for 8 days.

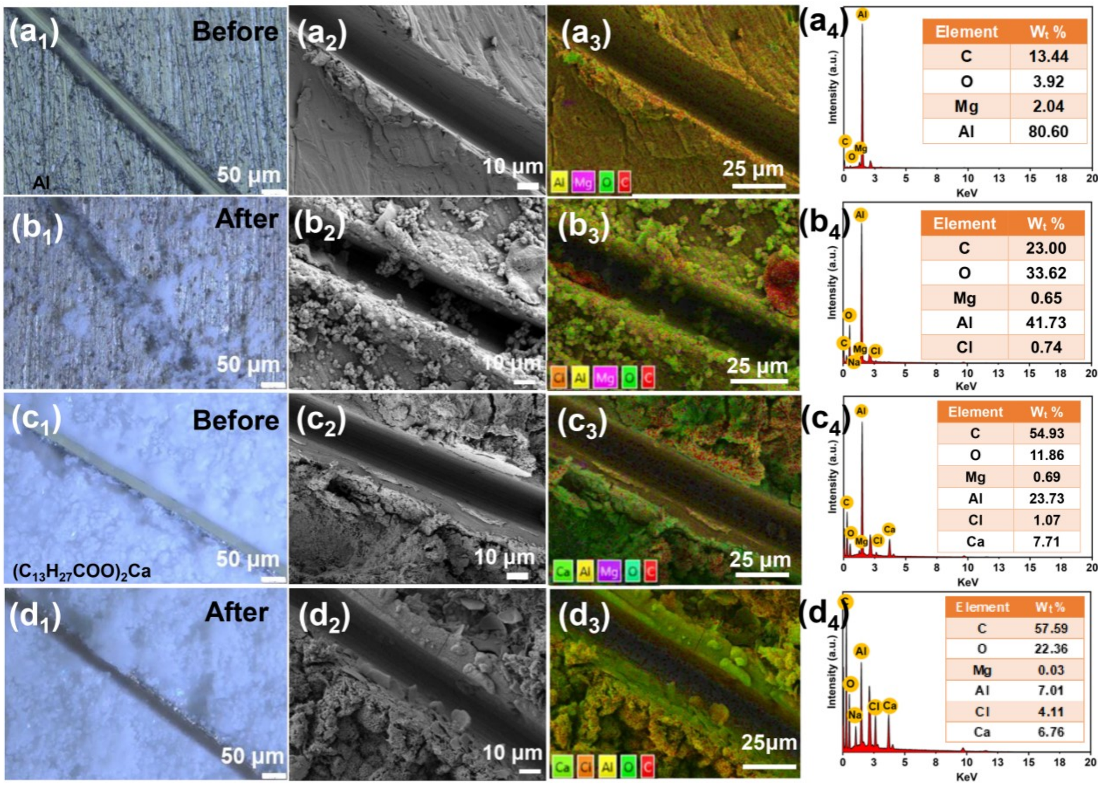

Fig. S24. Optical images, SEM images, EDS mappings, and atomic percentages of the scratched samples before and after immersion test for 192 h in 3.5 wt.% NaCl solution: (a_1-a_4) before and (b_1-b_4) after immersion tests for Al alloy, and (c_1-c_4) before and (d_1-d_4) after immersion test for $(C_{13}H_{27}COO)_2Ca$ coating.

Reference

[S1] X. Sun, S. Gu, L. Wang, H. Wang, S. Xiong, X. Yin, S. Yang, Multifunctional liquid-like magnetic nanofluids mediated coating with anticorrosion and self-healing performance, Journal of Colloid and Interface Science, 654 (2024) 25-35.

[S2] S. Liu, Z. Li, Q. Yu, Y. Qi, Z. Peng, J. Liang, Dual self-healing composite coating on magnesium alloys for corrosion protection, Chemical Engineering Journal, 424 (2021) 130551.

[S3] Y. Huang, T. Liu, L. Ma, J. Wang, D. Zhang, X. Li, Saline-responsive triple-action self-healing coating for intelligent corrosion control, Materials & Design, 214 (2022) 110381.

[S4] L. Cao, W. Wang, J. Cheng, T. Wang, Y. Zhang, L. Wang, W. Li, S. Chen, Synergetic Inhibition and Corrosion-Diagnosing Nanofiber Networks for Self-Healing Protective Coatings, ACS Applied Materials & Interfaces, 15 (2023) 48645-48659.

[S5] R. Wang, L. Cao, W. Wang, Z. Mao, D. Han, Y. Pei, Y. Chen, W. Fan, W. Li, S. Chen, Construction of Smart Coatings Containing Core–Shell Nanofibers with Self-Healing and Active Corrosion Protection, ACS Applied Materials & Interfaces, 16 (2024) 42748-42761.

[S6] X. Fu, W. Du, H. Dou, Y. Fan, J. Xu, L. Tian, J. Zhao, L. Ren, Nanofiber composite coating with self-healing and active anticorrosive performances, ACS Applied Materials & Interfaces, 13 (2021) 57880-57892.
[S7] L. Cheng, C. Liu, H. Wu, H. Zhao, F. Mao, L. Wang, A mussel-inspired delivery system for enhancing self-healing property of epoxy coatings, Journal of Materials Science & Technology, 80 (2021) 36-49.
[S8] Z. Bi, F. Gao, M. Liu, R. Zhang, R. Liu, G. Cui, J. Xu, Multifunctional self-healing coatings with orderly distributed microcapsules aligned by magnetic field, Chemical Engineering Journal, 450 (2022) 138250.
[S9] Q. Zhang, W. Li, X. Liu, J. Ma, Y. Gu, R. Liu, J. Luo, Polyaniline Microspheres with Corrosion Inhibition, Corrosion Sensing, and Photothermal Self-Healing Properties toward Intelligent Coating, ACS Applied Materials & Interfaces, 16 (2023) 1461-1473.
[S10] B. Li, D. Njuko, M. Meng, A. Tang, Y. Li, Designing smart microcapsules with natural polyelectrolytes to improve self-healing performance for water-based polyurethane coatings, ACS Applied Materials & Interfaces, 14 (2022) 53370-53379.

a